RESEARCH PAPER P-243

TIME AND FREQUENCY CHARACTERISTICS OF AN ACOUSTIC SIGNAL REFLECTED FROM A ROUGH BOUNDARY

John J. Martin

February 1966

INSTITUTE FOR DEFENSE ANALYSES
RESEARCH AND ENGINEERING SUPPORT DIVISION

RESEARCH PAPER P-243

TIME AND FREQUENCY CHARACTERISTICS OF AN ACOUSTIC SIGNAL REFLECTED FROM A ROUGH BOUNDARY

John J. Martin

February 1966

INSTITUTE FOR DEFENSE ANALYSES
RESEARCH AND ENGINEERING SUPPORT DIVISION

Contract SD-50
Task T-37

The ***Institute for Defense Analyses*** *produces three kinds of publication for distribution, entitled Report, Study, and Research Paper.*

A ***Report*** *embodies the results of a major research project undertaken by IDA and is intended to be an authoritative contribution on its subject.*

A ***Study*** *is a less formal document and less comprehensive in scope than a Report. It may be the result of a smaller and more narrowly defined research project or it may be a supporting technical paper prepared in connection with a major project.*

A ***Research Paper*** *represents the work of one or more named authors but is subject to review comparable to that for publication in a professional journal.*

ACKNOWLEDGMENT

It is a pleasure to acknowledge that the comments of Drs. J. A. Navarro and L. B. Wetzel were helpful in improving the presentation of the material contained in this Research Paper.

CONTENTS

FIGURES

NOMENCLATURE

SYMBOLS

$B(\ )$	correlation function
$B''(\ )$	correlation function second derivative
c	acoustic phase velocity; sound speed
E	expected value
Δf	doppler frequency (Appendix II)
J	Jacobian (Eq. 30)
N	number of multipaths or arrivals
$p(\cdot)$	probability
r	correlation distance
x	distance downrange from source
y	distance crossrange, normal to x-z
z	distance above reflecting bottom
θ	bottom slope
σ	standard deviation
v	speed
φ	acoustic ray angle to horizontal
$\Delta\tau$	pulse time

SUBSCRIPTS

ℓ	lower
M	multipath
max	maximum
min	minimum
o	surface to bottom or reference value
R	receiver/reflector
S	source
R	round-trip
u	upper
z	elevation
θ	slope
1	outgoing or one-way
2	returning
c	center

I. INTRODUCTION

The reflection of acoustic energy by a rough surface, such as the ocean bottom, is of practical interest. If the acoustic signals propagated in such a manner occur between moving source and receiver or reflector, and if the reflecting boundary is not-too-rough,* then, due to a single pulse, there may be numerous more or less discrete "arrivals" (Refs. 1,2) at both terminals of the propagation path. These arrivals which may have an associated doppler shift in frequency arrive along various "multipaths." In signal-processing techniques using time and frequency correlation, an understanding of relationships among kinematic, geometric, and environmental aspects of such a problem is essential. This paper presents an analysis for determining on a statistical basis expected acoustic signal arrival times and corresponding expected doppler frequency shifts for both one-way and round-trip paths. There may also be an ionospheric radar application.

This paper proceeds by analyzing the transit time and doppler frequency characteristics of a narrow pulse on one-way multipaths from a sea bottom with random normal distribution of slope but negligibly

*A not-too-rough surface is one which has variances of surface elevation derivatives sufficiently small that there is no appreciable occultation of surface area at oblique incidence angles; as a related practical matter in transmitting energy to a receiver or reflector, it is necessary that surface correlation lengths be sufficiently great that at least the first Fresnel zone is nominally flat.

large bottom elevation variance; it continues--through a convolution of this "one-way" case--by determining the properties of narrow pulses on round-trip multipaths; next, this round-trip, narrow pulse analysis is extended to long pulses and, finally, the importance of non-negligible bottom elevation variance and source and receiver-reflector motion is considered.

II. ANALYSIS

A. ONE-WAY PATHS, NARROW PULSE

Let Fig. 1 represent one of a number of one-way paths between a moving acoustic source, S, and a moving receiver, R, i.e., a narrow pulse transmitted from S is received at R intentionally (communicating) or unintentionally (interferring). The analysis is restricted for now to narrow (delta-function) pulses for simplicity but the more general finite width pulse will be treated subsequently with a measure of "narrow" given then. In this, θ is the local slope of the reflecting boundary which is presumed to have correlation lengths of bottom elevation and its first two derivatives very large relative to the wavelength of the acoustic energy. As a concomitant of this, it is presumed also that bottom elevation variance is unimportant. As this latter assumption will not always be valid, the effect of importantly large elevation variance is treated in a subsequent section. For the sake of simplicity in discussing the problem, only one-dimensional roughness in the direction of propagation will be considered; extension to two-dimensional roughness is possible though tedious (Appendix I). The one-dimensional problem is reasonably descriptive of the two-dimensional situation because the probability of paths at large azimuthal excursions from the plane of Fig. 1 is small (Ref. 2) for typical sea bottom, and this being so, the signal transit time and

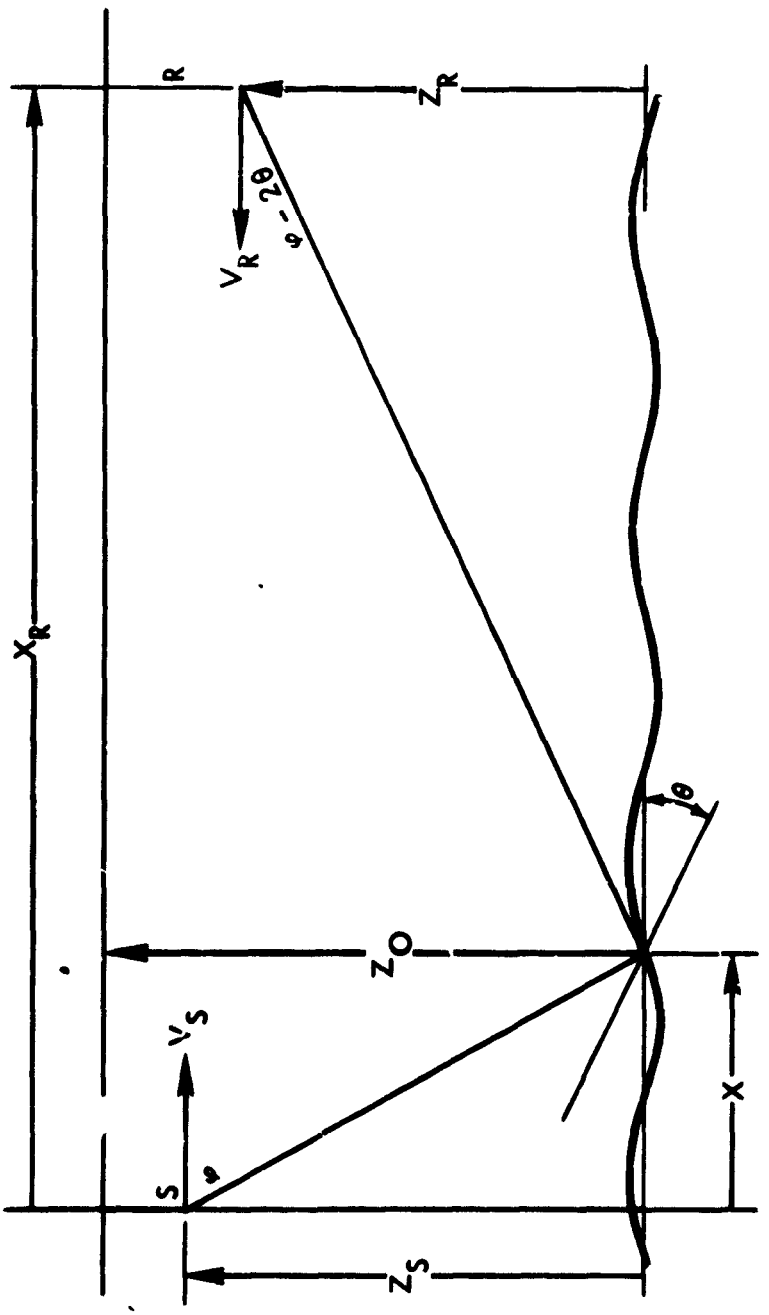
R
Z_R
V_R
$\varphi - 2\theta$
X_R
θ
Z_O
V_S
S
φ
X
Z_S

doppler frequency between S and R are determined with only small error by in-plane components.

Now in Fig. 1, the relationships among the several variables is as follows:*

$$x = z_s \cot \varphi \tag{1A}$$

$$x_R - x = z_R \cot (\varphi - 2\theta) \tag{1B}$$

from which it develops that a ray from S will reflect to R if

$$\theta = \theta_M = \frac{1}{2} \left[\varphi - \operatorname{arccot} \left(\frac{x_R - z_s \cot \varphi}{z_R} \right) \right] \tag{2}$$

where the subscript M indicates that a multipath exists between S and R as a function of φ, z_s, z_R, and x_R. It has been shown (Refs. 1,2; Appendix I) that if θ has a Gaussian, i.e., normal distribution then the probable or expected number of multipaths in an increment of bottom distance x is

$$p(M \text{ in } dx: \varphi, z_s, z_R, x_R) \equiv dE(N_1) = \frac{1}{\pi} \left[- \frac{B_\theta''(0)}{B_\theta(0)} \right]^{\frac{1}{2}} \exp (-\theta_M^2/2\sigma_\theta^2)\, dx \tag{3}$$

It may be mathematically more satisfying to assume tan θ as having Gaussian distribution; if $\sigma_\theta \ll 1$ it makes little difference which assumption is made, although as $\theta \leq \tan \theta$, Gaussian θ yields greater

*If index of refraction variation is, on the average, important then this analysis must be modified (Ref. 2).

expected values as is clear from Eq. 3. Presently, experimental data are insufficient to make a decision between the two assumptions and a Gaussian distribution of θ is used to simplify calculation.

Now the expected number of multipaths in dx may, using Eqs. 1A and 3, be transformed to the expected angular density of one-way multipaths $E(N_1)$ as

$$\frac{dE(N_1)}{d\varphi} = -\left(\frac{z_s}{\pi}\right)\left[-\frac{B''_\theta(0)}{B_\theta(0)}\right]^{\frac{1}{2}} \csc^2\varphi \exp\left(-\theta_M^2/2\sigma_\theta^2\right) \qquad (4)$$

In anticipation of determining transit time and doppler frequency of multipath arrivals, the cumulative expected number of multipaths $E_1^*(\varphi)$ between $\varphi = 0^+$ deg and φ is determined from Eq. 4 as

$$E_1^*(\varphi) = \int_{0^+}^{\varphi}\left[\frac{dE(N_1)}{d\varphi}\right] d\varphi \qquad (5)$$

the integration being carried from $\varphi = 0^+$ to avoid a singular point at $\varphi = 0$ which arises from using θ rather than $\tan\theta$ in Eq. 3.

Given the conditions described graphically in Fig. 1, signal transit time and doppler frequency may be determined. From Fig. 1 the one-way signal transit time of narrow pulses is

$$t_1/(z_s/c) = \left[\csc\varphi + (z_R/z_s)\csc(\varphi - 2\theta)\right] \qquad (6)$$

and the one-way doppler frequency is, approximately (Appendix II)

$$\left[\frac{(\Delta f_1/f_o)}{v_s/c}\right] \cong \cos\varphi + (v_R/v_s)\cos(\varphi - 2\theta) \tag{7}$$

In Eqs. 6 and 7, c is sound speed, f_o the at-rest frequency of the sound propagation of S and it is assumed that v_s and v_R are positive as shown in Fig. 1. Figure 2 shows $E_1^*(\varphi)$, $t_1(\varphi)$ and $\Delta f_1(\varphi)$ for the following values of parameters to be used in this paper unless otherwise noted:

$$\begin{aligned}
x_R/z_s &= 5.5 \\
z_s = z_R &= 2200 \text{ fathoms} = 13{,}200 \text{ ft} = 4024 \text{ m} \\
v_s = v_R &= 0.01\ c \\
c &= 5000 \text{ fps} = 2961 \text{ knots} = 1524 \text{ m/sec} \\
\varphi_o &= \operatorname{arccot}[x_R/(z_s + z_R)] = 20 \text{ deg} \\
\varphi_{min} &= 15 \text{ deg} \\
\varphi_{max} &= 25 \text{ deg} \\
\sigma_\theta &= 3.75 \text{ deg} = 0.0655 \text{ radian} \\
[-B_\theta''(0)/B_\theta(0)]^{\frac{1}{2}} &= (1025 \text{ ft})^{-1} = (312.5 \text{ m})^{-1}
\end{aligned} \tag{8}$$

Figure 2 has special utility in that if transmission from S is between φ_{min} and φ_{max} only, then for this beamwidth the expected number of one-way multipaths between S and R is just $E_1^*(\varphi_{max}) - E_1^*(\varphi_{min})$.

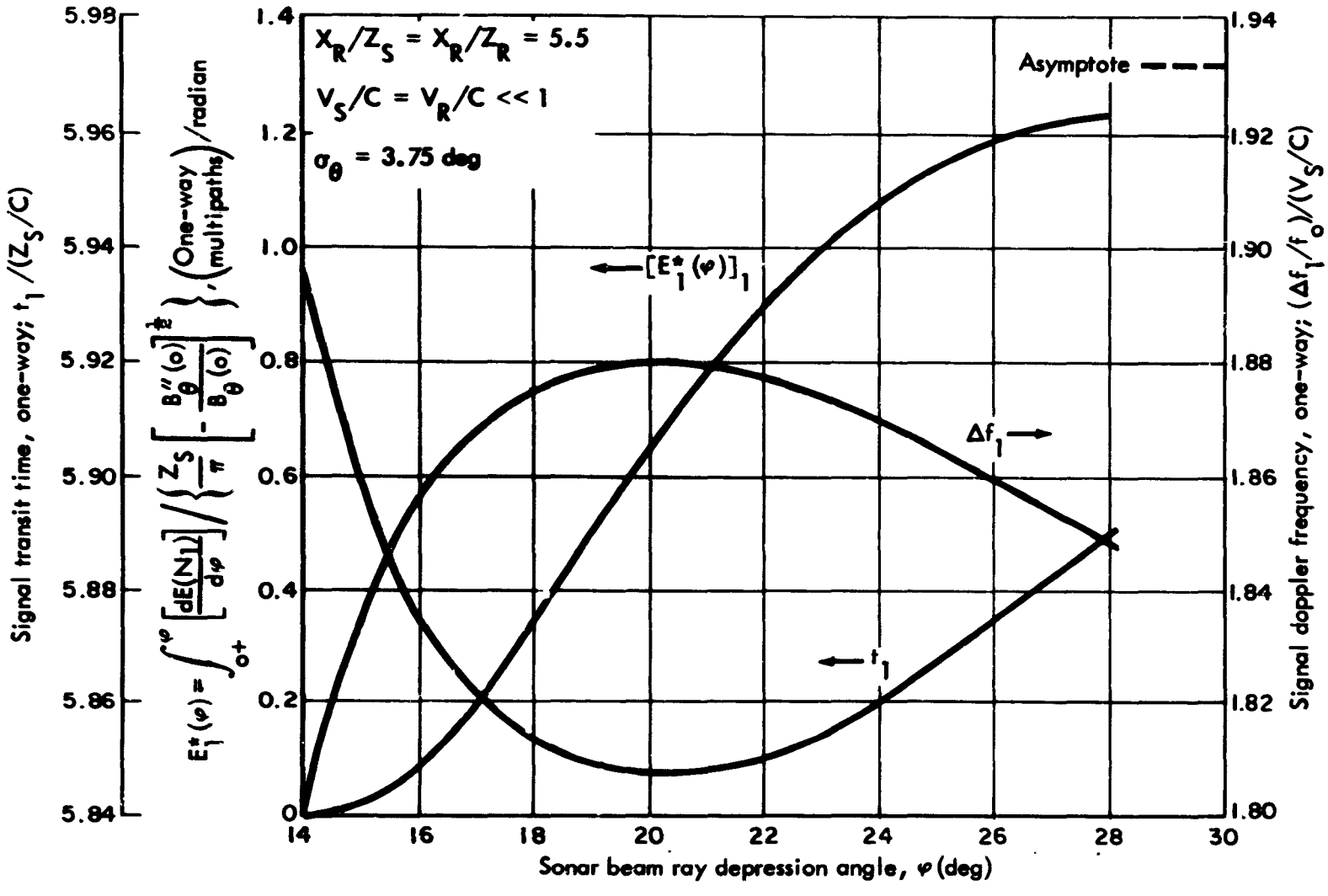

FIGURE 2 One-Way Multipath Expected Number, Transit Time and Doppler Frequency--Narrow Pulse

1. Multipath Maximum Number for Fixed Beamwidth

Equation 5 which gives an expression for expected number of multipaths may be used to determine beam depression to maximize the number of arrivals at R from S for a given beamwidth, $\Delta\varphi$. Consider

$$E(N_1) = \left(\frac{z_s}{\pi}\right)\left[-\frac{B_\theta''(0)}{B_\theta(0)}\right]^{\frac{1}{2}} \int_{\varphi_c - \frac{1}{2}\Delta\varphi}^{\varphi_c + \frac{1}{2}\Delta\varphi} - \csc^2\varphi \exp\left[-(\theta_M^2/2\sigma_\theta^2)\right] d\varphi \quad (9)$$

where $\Delta\varphi$ is a fixed beamwidth and φ_c is the beam center. If Eq. 9 be differentiated with respect to φ_c and set equal to zero, then there results the condition for which $E(N_1)$ is maximized as a function of φ_c.

Using Leibnitz rule, the derivative of Eq. 9 with respect to φ_c is

$$\frac{dE(N_1)}{d\varphi_c} = -\left(\frac{z_s}{\pi}\right)\left[-\frac{B_\theta''(0)}{B_\theta(0)}\right]^{\frac{1}{2}} \Big\{\csc^2(\varphi_c + \tfrac{1}{2}\Delta\varphi) \exp\left[-\theta_M^2(\varphi_c + \tfrac{1}{2}\Delta\varphi)/2\sigma_\theta^2\right] - \csc^2(\varphi_c - \tfrac{1}{2}\Delta\varphi) \exp\left[-\theta_M^2(\varphi_c - \tfrac{1}{2}\Delta\varphi)/2\sigma_\theta^2\right] + 0\Big\} \quad (10A)$$

If this derivative be set equal to zero there results

$$\csc^2(\varphi_c + \tfrac{1}{2}\Delta\varphi) \exp\left[-\theta_M^2(\varphi_c + \tfrac{1}{2}\Delta\varphi)/2\sigma_\theta^2\right] = \csc^2(\varphi_c - \tfrac{1}{2}\Delta\varphi) \exp\left[-\theta_M^2(\varphi_c - \tfrac{1}{2}\Delta\varphi)/2\sigma_\theta^2\right] \quad (10B)$$

which by reference to Eq. 4 is simply the condition that $\left[\frac{dE(N_1)}{d\varphi}\right]_{\varphi_{max}} = \left[\frac{dE(N_1)}{d\varphi}\right]_{\varphi_{min}}$. In other words, for a given beamwidth $\varphi_{max} - \varphi_{min} = \Delta\varphi$, the number of multipaths within $\Delta\varphi$ will maximize when the angular density of multipaths at the beam's edges are equal; generally $\varphi_o \neq \text{arccot}\,[x_R/(z_s + z_R)] = \varphi_o$, the apparent specular point.

2. Doppler Frequency Mean-Slope Deviation Relationship*

A measure of surface slope standard deviation from the doppler frequency mean devolves from the case in which S follows R at fixed x_R, i.e., $|v_s| = |v_R|$. Then, for θ small, doppler frequency is given by

$$\left[\frac{(\Delta f_1/f_o)}{(v_s/c)}\right] \cong \cos\varphi - c\,\text{s}\,(\varphi - 2\theta) \cong -2\theta \sin\varphi \tag{11}$$

and for this condition the expected value of the absolute deviation of doppler shift is, for σ_θ small also

$$E\left[\left|\frac{(\Delta f_1/f_o)}{(v_s/c)}\right|\right] = 2\int_o^{\pi/2} \frac{2\theta \sin\varphi}{\sqrt{2\pi}\,\sigma\theta} \exp\left(-\theta^2/2\sigma_\theta^2\right) d\theta \tag{12}$$

*What follows may bear some pertinence also to an electromagnetic source and its receiver moving relative to a randomly refracting ionosphere.

where $\varphi = \varphi(\theta)$ from Eq. 2. If a mean value of $\overline{\varphi} \cong \varphi_o \equiv \text{arccot}\ x_R/(z_s + z_R)$ is used, then

$$E\left[\left|\frac{(\Delta f_1/f_o)}{(v_s/c)}\right|\right] \cong \frac{4\sigma_\theta \sin \varphi_o}{\sqrt{2\pi}} \tag{13}$$

i.e.,

$$E|(\Delta f_1)| \cong 2\sqrt{2/\pi}\,(v_s/c) f_o \sigma_\theta \sin \varphi_o \tag{14}$$

Apparently, therefore, mean doppler shift is a direct measure of ocean bottom roughness variance; for conditions of Eq. 8, Eq. 14 takes a value of 0.2 cps/kcps. A related result is obtained if $\langle(\Delta f_1)^2\rangle$ is determined instead of $\langle|\Delta f_1|\rangle$.

3. Transit Time and Doppler Frequency Characteristics

Figure 2 and the analysis leading to it provide a basis for describing some of the statistical characteristics of signal transit time and doppler frequency. Generally, the expected number of arrivals until t_1' is

$$\left[E(N_1)\right]_{t_1 \le t_1'} = \int_{\varphi_\ell(t_1')}^{\varphi_u(t_1')} \left[\frac{dE(N_1)}{d\varphi}\right] d\varphi \tag{15}$$

where $\varphi_u(t_1') > \varphi_o$ and $\varphi_\ell(t_1') < \varphi_o$ are angles appropriate, as in Fig. 2, to a transit time t_1'. Thus the time rate of arrivals is just the

derivative of Eq. 15 which, using Leibnitz rule, is (with primes omitted)*

$$\frac{dE(N_1)}{dt_1} = \left\{\left[\frac{dE(N_1)}{d\varphi}\right]\left(\frac{d\varphi}{dt_1}\right)\right\}_{\varphi_u(t_1)} - \left\{\left[\frac{dE(N_1)}{d\varphi}\right]\left(\frac{d\varphi}{dt_1}\right)\right\}_{\varphi_\ell(t_1)} \tag{16}$$

where $\varphi_{min} \le \varphi_\ell(t_1) < \varphi_o$ and $\varphi_o < \varphi_u(t_1) \le \varphi_{max}$, $\varphi_o = \text{arccot}\ x_R/(z_s + z_R)$; if $\varphi_\ell(t_1) < \varphi_{min}$ or if $\varphi_u(t_1) > \varphi_{max}$ then $d\varphi/dt_1 \equiv 0$.

The expected number of arrivals from S at R prior to a given time t_1' is available in an alternative form from Eq. 16 by integration; thus

$$\left[E(N_1)\right]_{t_1 \le t_1'} = \int_{t_{min}}^{t_1'} \left[\frac{dE(N_1)}{dt_1}\right] dt_1 \tag{17}$$

where the integrand of Eq. 17 comes from Eq. 16 with the associated restrictions, and t_{min} is the least transit time appropriate to the beam, $(\varphi_{max}, \varphi_{min})$. Clearly

$$\lim_{t_1' \to \infty} \int_0^{t_1'} \left[\frac{dE(N_1)}{dt_1}\right] dt_1 \equiv \int_{\varphi_{min}}^{\varphi_{max}} \left[\frac{dE(N_1)}{d\varphi}\right] d\varphi \tag{18}$$

A parallel construction for doppler frequency characteristics is possible and one may write straightforwardly the analog of Eq. 16 as

---

*It is assumed that $dx_R/dt = 0$ as a consequence of small v_s and v_R; this introduces a negligible error.

$$\frac{dE(N_1)}{d\Delta f_1} = \left\{\left[\frac{dE(N_1)}{d\varphi}\right]\left(\frac{d\varphi}{d\Delta f_1}\right)\right\}_{\varphi_\ell(\Delta f_1)} - \left\{\left[\frac{dE(N_1)}{d\varphi}\right]\left(\frac{d\varphi}{d\Delta f_1}\right)\right\}_{\varphi_u(\Delta f_1)} \qquad (19)$$

where $\varphi_{min} \leq \varphi_\ell(\Delta f_1) < \varphi_o'$ and $\varphi_o' < \varphi_u(\Delta f_1) \leq \varphi_{max}$. In this $\varphi_o' = \varphi[(\Delta f_1)_{max}]$ from Eq. 7; again if φ_ℓ and φ_u lie outside the interval $(\varphi_{min}, \varphi_{max})$ then $\left(\frac{d\varphi}{d\Delta f_1}\right) \equiv 0$.

The expected number of arrivals from S at R with doppler frequency less than a given value $\Delta f_1'$ is, in parallel with Eq. 17,

$$\left[E(N_1)\right]_{\Delta f_1 \leq \Delta f_1'} = \int_0^{\Delta f_1'} \left[\frac{dE(N_1)}{d\Delta f_1}\right] d\Delta f_1 \qquad (20)$$

The transit time and doppler frequency characteristics of the signals are not independent as Fig. 2 suggests: For a given one-way path arrival time, one of two possible sonar beam depression angles is permissible, in general, and the doppler frequency is fixed by these angles. Hence for one-way transmission, doppler frequency is one of two values fixed by arrival time.

Figure 3 shows the cumulative number of "arrivals," i.e., multipaths of a single very narrow pulse as a function of time and doppler frequency. For the typical values of Eq. 8, numerical values from Fig. 2 are

maximum number of multipaths or "arrivals":

$$\left[E(N_1)\right]_{max} = 1.32 \left(\frac{13{,}200 \text{ ft}}{\pi}\right)\left(1025 \text{ ft}\right)^{-1} = 5.4$$

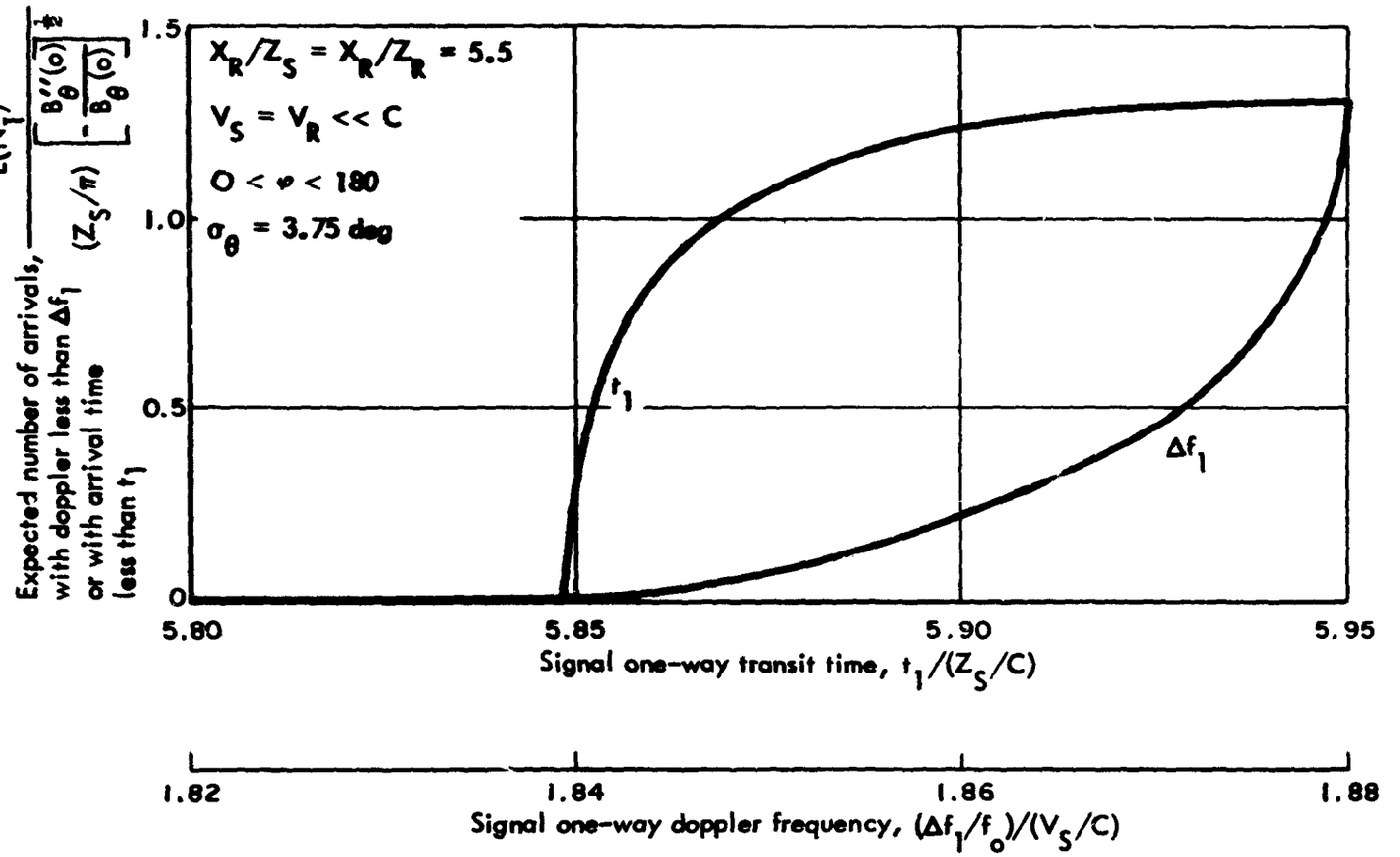

FIGURE 3 One-Way Multipath Transit Time and Doppler Frequency Cumulative Density--Narrow Pulse

and from Fig. 3,

time interval of 50 percent of the arrivals:

$$(\Delta t)_{0.5} = (5.854 - 5.848)\ \frac{13{,}200\ \text{ft}}{5000\ \text{fps}} \approx 15.8\ \text{msec}$$

Figure 2 indicates that

maximum doppler frequency $(\Delta f_1)_{max}$:

$$\left(\frac{\Delta f_1}{f_o}\right)_{max} = 1.88\ \left(\frac{50\ \text{fps}}{5000\ \text{fps}}\right) = 18.8\ \text{cps/kcps of } f_o$$

and Fig. 3 shows

frequency interval of 90 percent of the arrivals:

$$\Delta\left[\left(\frac{\Delta f_1}{f_o}\right)\right]_{0.9} = (1.880 - 1.8535)\ \left(\frac{50\ \text{fps}}{5000\ \text{fps}}\right) = 0.265\ \text{cps/kcps of } f_o$$

i.e., substantially all the arrivals have doppler frequency between 18.5 and 18.8 cps/kcps for R closing on S each at one percent sound speed, and for typical geometry and ocean bottom conditions.

The situation which Fig. 2 typifies may be elaborated. If S is not transmitting omnidirectionally ($0 \leq \varphi \leq 180$ deg) but is limited ($\varphi_{min} \leq \varphi \leq \varphi_{max}$) then the expected number of multipaths to R may as stated be determined as the difference $E_1^*(\varphi_{max}) - E_1^*(\varphi_{min})$ for this latter case. The distributions of Fig. 3 will, of course, be modified by this, but these actual distributions may be determined from Fig. 2

with care for beam limits. If further, R is "listening" with a limited beam then the number of multipaths and their time and frequency characteristics will be determined by the interval Δx of ocean bottom which is common to the beamwidths of both S and R. Finally, if the upper bounding surface is planar for waves of frequency f_o (Ref. 3) then the number of paths to R from S via the surface may be determined by replacing z_R in the foregoing by $2z_o - z_R$ (the distance above the bottom of the virtual receiver). If $(z_o - z_R)/z_o \ll 1$ then the number of paths via the bottom and surface is approximately that via the bottom alone, and the arrival time and doppler frequency characteristics will be similar also for the two path types. Hence for this situation, numbers of arrival and densities of arrivals in time and frequency will be approximately doubled.

B. ROUND-TRIP PATHS, NARROW PULSE

The treatment above of one-way paths provides the basis for determining the expected number, transit time, and doppler frequency of round-trip paths for sound waves reflected from a not-too-rough boundary. Figure 4 gives the geometry and nomenclature for this round-trip case which is a straightforward elaboration of Fig. 1.

Now if $p(M \text{ in } dx_1 : \varphi_1, z_s, z_R, x_R)$ is the probable number of outgoing multipaths occurring in dx_1, and $p(M \text{ in } dx_2 : \varphi_2, z_s, z_R, x_R)$ is the corresponding number of a return path occurring in dx_2, then the probable number of round-trip paths as a result of reflection at R going through dx_1 and dx_2 is the product of these individual incremental numbers and

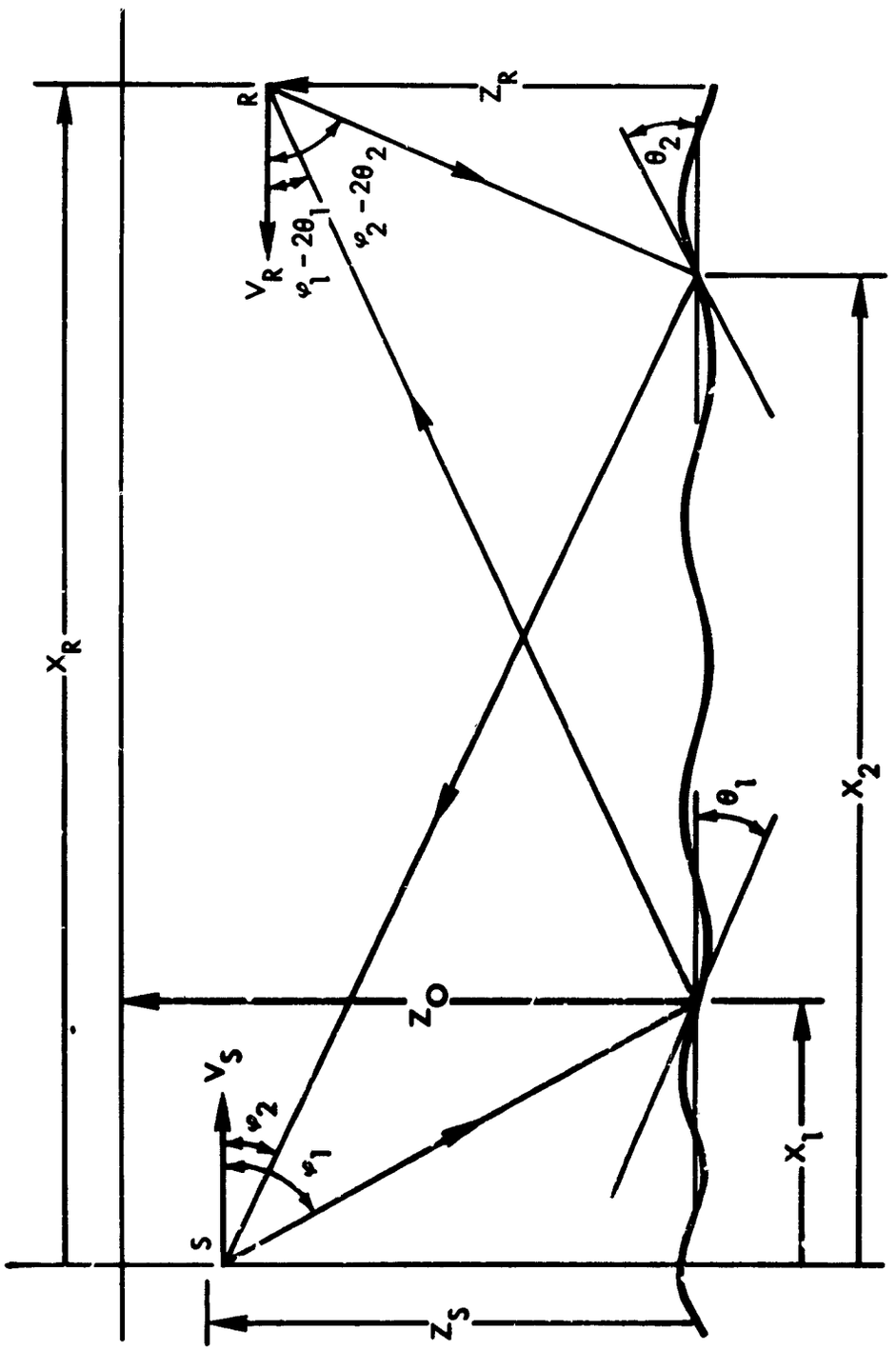

FIGURE 4 Round-Trip Bottom Bounce Propagation Geometry

$$d^2E(N_2) = \left[\frac{dE(N_1)}{dx_1}\right]\left[\frac{dE(N_1)}{dx_2}\right] dx_1\ dx_2 \tag{21}$$

The expected number $E(N_2)$ of round-trip paths between S and R is the integral of Eq. 21, i.e.,

$$E(N_2) = \int_{\Delta x_1}\int_{\Delta x_2} d^2E(N_2) \tag{22}$$

or in explicit form as a function of beam depression angle

$$E(N_2) = \left(\frac{z_s}{\pi}\right)^2 \left[-\frac{B_\theta''(0)}{B_\theta(0)}\right] \int_{(\varphi_1)_{min}}^{(\varphi_1)_{max}} \int_{(\varphi_2)_{min}}^{(\varphi_2)_{max}} \csc^2\varphi_1\ \csc^2\varphi_2$$
$$\exp\left\{-\frac{1}{2}\left[\left(\theta_M/\sigma_\theta\right)_1^2 + \left(\theta_M/\sigma_\theta\right)_2^2\right]\right\} d\varphi_1\ d\varphi_2 \tag{23}$$

As φ_1 and φ_2 and independent, if R is ensonified and reflects only in the two downward quadrants and if the transmitting and receiving beams at S are identical, then from Eqs. 4 and 23

$$E(N_2) = \left[E(N_1)\right]^2 \tag{24}$$

If, however, R is ensonified from both planar surface and rough bottom and can reflect these arrivals in either the bottom or surface-bottom paths, then the total expected number of multipaths may be as large as $4[E(N_1)]^2$. For the example of the preceeding section for one-way paths

with $z_R \cong z_o$, this takes a value of $4(5.4)^2 > 116$, not to be sure, all of the same intensity. Figure 5 shows the density of multipaths in transmit-angle (φ_1) and receive-angle (φ_2) space based on the integrand of Eq. 23 and it is interesting that the maximum angular density occurs for $\varphi \cong 18.7$ degrees, at lesser depression than the "specular" angle $\varphi_o = 20$ degrees. Figure 5 is, of course, a two-dimensional representation of a surface and provides a basis for considering the transit time and doppler frequency characteristics of round-trip multipaths and their density distribution in time-frequency space.

The round-trip transit time t_R of a narrow pulse is

$$t_R = t_1 + t_2 \tag{25}$$

where

$$t_i/(z_s/c) = [\csc \varphi_i + (z_R/z_s) \csc (\varphi_i - 2\theta_i)], \; i = 1,2$$

Thus once the geometry of Fig. 4 is fixed, $t_i = t_i(\varphi_i)$. The round-trip doppler frequency is

$$\Delta f_R = \Delta f_1 + \Delta f_2 \tag{26}$$

where there is associated with each direction a doppler frequency given approximately as (see Appendix II)

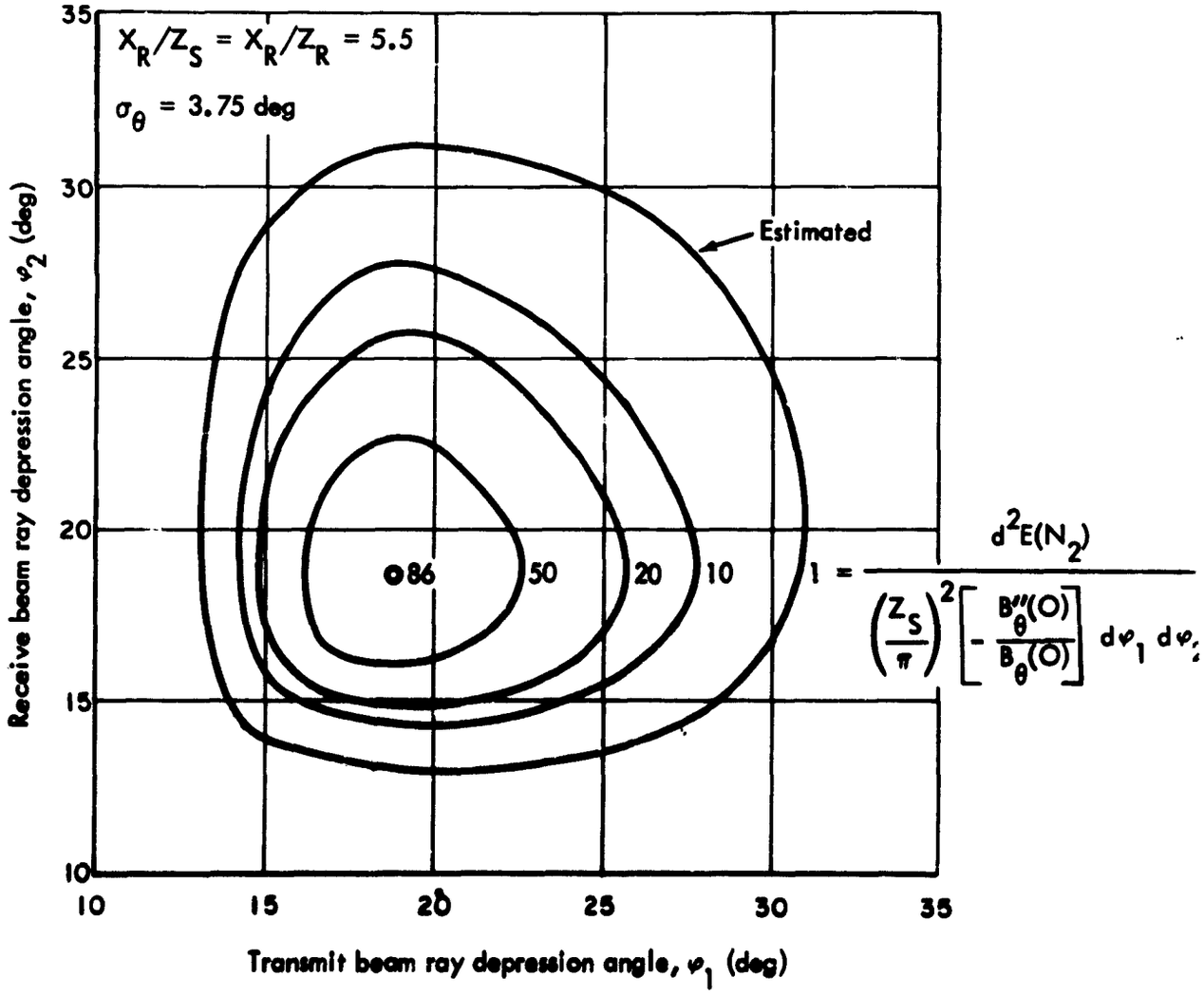

FIGURE 5 Round-Trip Multipath Density in Transmit--and Receive-Beam Angle Space--Narrow Pulse

$$\left[\frac{(\Delta f_i / f_o)}{(v_s/c)}\right] = \left[\cos \varphi_i + (v_R/v_s) \cos (\varphi_i - 2\theta_i)\right], \quad i = 1,2$$

and again $\Delta f_i = \Delta f_i (\varphi_i)$.

Given the foregoing equations, it is of interest at first to describe the arrival rate of a narrow pulse on round-trip paths. Now the probability of an arrival during dt_R' is just the probability of an arrival at R during dt_1 multiplied by the probability of an arrival at S from R during $dt_2 = d(t_R' - t_1)$, summed over all $t_R' = t_1 + t_2$. This is shown schematically in Fig. 6. Thus

$$p(M \text{ in } dt_R') = \int_{(t_1)_{min}}^{t_R' - (t_2)_{min}} p(M \text{ in } dt_1)\, p(M \text{ in } dt_2)\, dt_1 \qquad (27)$$

or, omitting primes

$$\left(\frac{dE(N_2)}{dt_R}\right) = \int_{(t_1)_{min}}^{t_R - (t_2)_{min}} \left[\frac{dE(N_1)}{dt_1}\right]_{t_1} \left[\frac{dE(N_1)}{dt_1}\right]_{t_R - t_1} dt_1 \qquad (28)$$

with the constraint that all of the interval t_1, t_2 lies within the interval φ_{min}, φ_{max}. Considering the complexity of the relationships among t_1, t_2 and φ_1, φ_2, it is likely that the maximum of Eq. 28 is most readily found through numerical integration of that equation. A construction similar to Eqs. 27 and 28 yields for dopper frequency

$$\left[\frac{dE(N_2)}{d\Delta f_R}\right] = \int_{\Delta f_R - (\Delta f_2)_{max}}^{(\Delta f_1)_{max}} \left[\frac{dE(N_1)}{d\Delta f_1}\right]_{(\Delta f_1)} \left[\frac{dE(N_1)}{d\Delta f_1}\right]_{\Delta f_R' - \Delta f_1} d\Delta f \qquad (29)$$

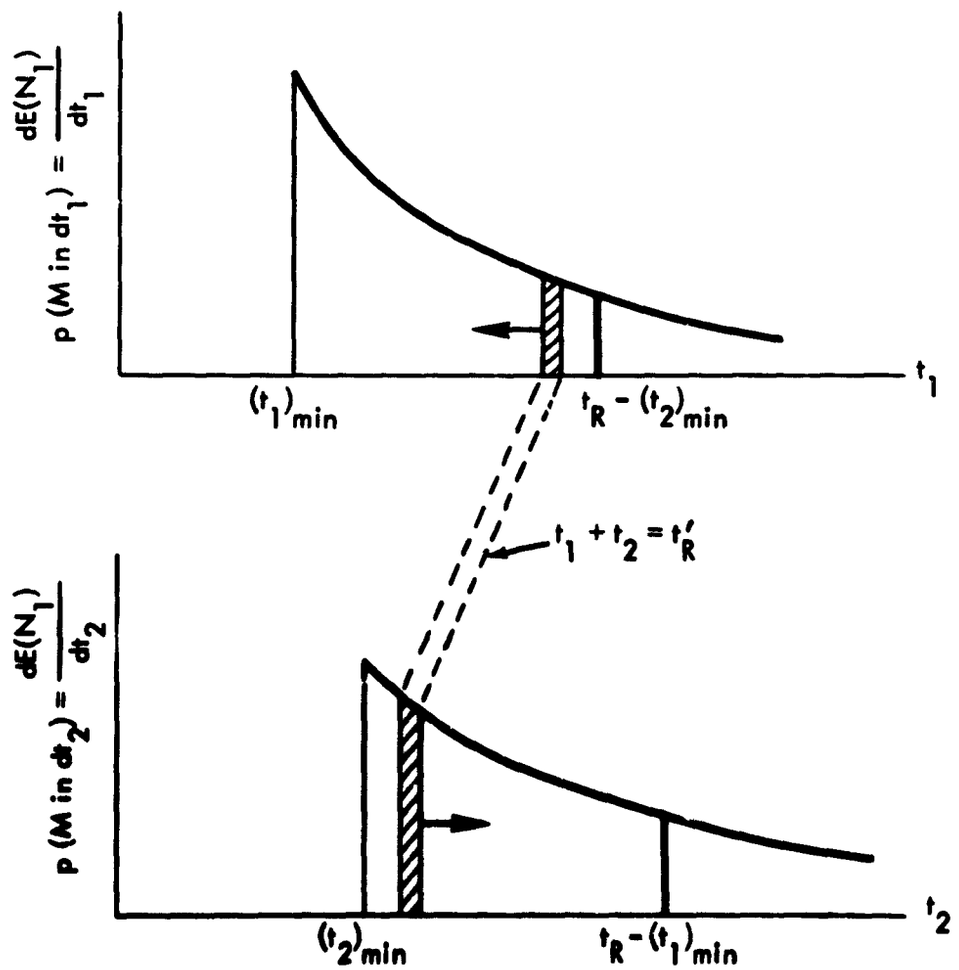

FIGURE 6 Schematic for Round-Trip Multipath Transit-Time Calculation--Narrow Pulse

and the maximum of this may again be found numerically. Figure 7 (obtained by graphical calculation and subject therefore to some error) shows the time and frequency distributions resulting from Eqs. 28 and 29. For the parametric values of Eq. 8, the interesting points of Fig. 7 are:

transit time t_R for maximum arrival rate: $(t_R)_{max\ rate}$

$$(t_R)_{max\ rate} - (t_R)_{min} \cong (11.699 - 11.695)\ (13{,}200/5000) = 16 \text{ msec}$$

maximum rate of arrivals:

$$\frac{dE(N_R)}{dt_R} \cong 58 \left[(13{,}200)(5000)/\pi^2\right] (1025 \text{ ft})^{-2} = 0.37/\text{msec}$$

doppler frequency corresponding to maximum spectral density:

$$\frac{\Delta f_R}{f_o} \cong 3.757\ (50 \text{ fps}/5000 \text{ fps}) = 37.57 \text{ cps/kcps of } f_o$$

maximum spectral density of arrivals:

$$\frac{dE(N_R)}{d(\Delta f_R)} \cong \left(\frac{52}{f_o}\right)\left(\frac{5000 \text{ fps } 13{,}200^2 \text{ ft}}{50 \text{ fps } \pi^2}\right)\left(1025\right)^{-2} \cong 0.9(10)^6/f_o$$

The time and frequency distributions of Fig. 7 are each without relation to the other. Thus one may desire the arrival density

$0 < \varphi < 180$ deg

$X_R/Z_S = X_R/Z_R = 5.5$

$V_S = V_R << C$

$\sigma_\theta = 3.75$ deg

N.B.: Portions of curves shown represent approximately 80 percent total round trip arrivals

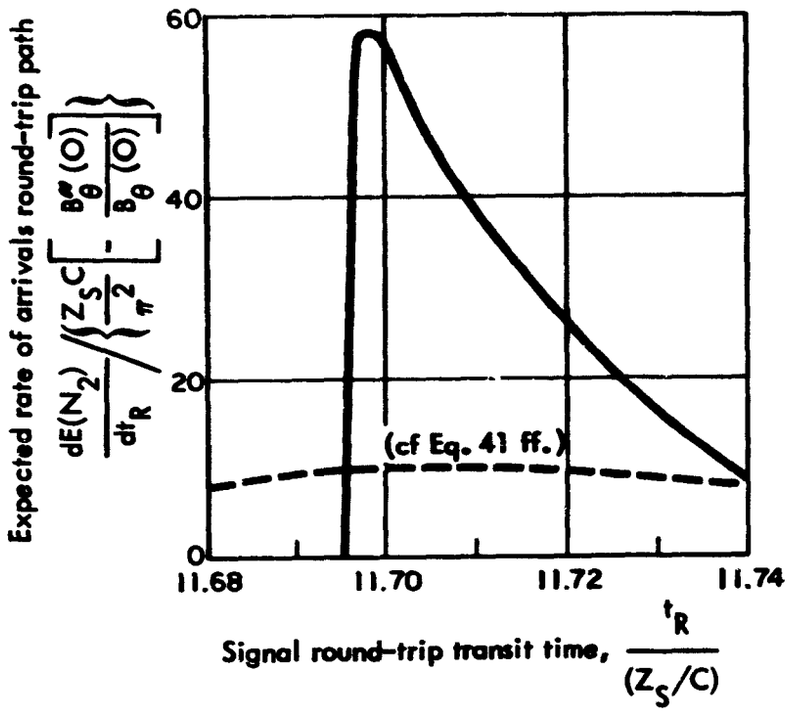

FIGURE 7A Multipath Cumulative Density vs. Transit Time--Narrow Pulse

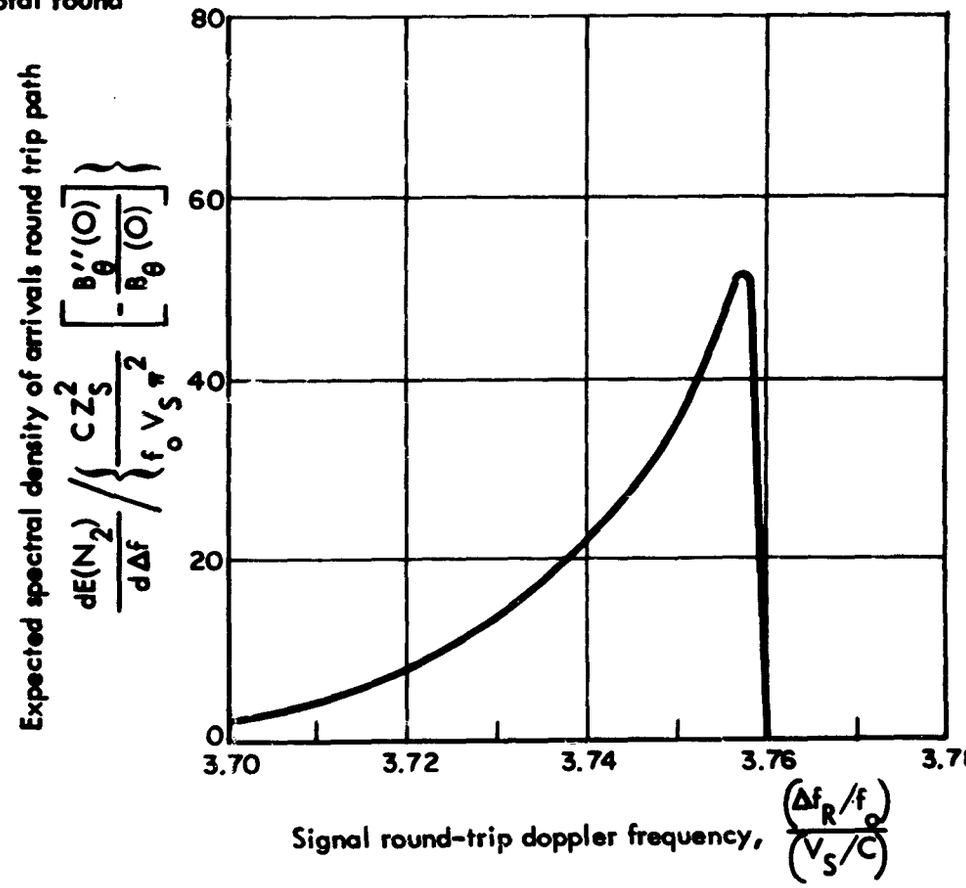

FIGURE 7B Multipath Cumulative Density vs. Doppler Frequency--Narrow Pulse

distributed in both time and frequency. Equation 21 may be transformed from (x_1, x_2)-space to $(t_R, \Delta f_R)$-space through the Jacobian; thus

$$d^2E(N_2) = \left[\frac{dE(N_1)}{dx_1}\right]\left[\frac{dE(N_1)}{dx_2}\right]\left|J\,\frac{(x_1, x_2)}{(t_R, \Delta f_R)}\right| dt_R\, d\Delta f_R \qquad (30)$$

where

$$\left|J\,\frac{(x_1, x_2)}{(t_R, \Delta f_R)}\right| \equiv \begin{vmatrix} \frac{\partial x_1}{\partial t_R} & \frac{\partial x_2}{\partial t_R} \\ \frac{\partial x_1}{\partial \Delta f_R} & \frac{\partial x_2}{\partial \Delta f_R} \end{vmatrix}$$

It may, however, be more convenient to write Eq. 30 as a function of (φ_1, φ_2) rather than (x_1, x_2). Equation 30 represents a surface over the $(t_R, \Delta f_R)$ plane, the height of which measures the density of arrivals as a function of time and doppler frequency. If Eq. 30 be written

$$\frac{d^2E(N_2)}{dt_R\, d\Delta f_R} = \left[\frac{dE(N_1)}{dx_1}\right]\left[\frac{dE(N_1)}{dx_2}\right]\left|J\,\frac{(x_1, x_2)}{(t_R, \Delta f_R)}\right| \qquad (31)$$

then if Eq. 31 be evaluated at $\Delta f_R = \Delta f_R'$ (a constant), there results the time rate of arrivals per unit doppler frequency at $\Delta f_R'$. Conversely, if Eq. 31 be evaluated at $t_R = t_R'$ (a constant), there results the spectral density of arrivals per unit time at t_R'. The surface represented by Eq. 31 is shown for typical values of bottom-bounce

geometry (Eq. 8) in Fig. 8. In this figure, in $(t_R, \Delta f_R)$-space not enclosed by the zero contour arrivals are impossible; the lines of infinite arrival density are a set of measure zero in $(t_R, \Delta f_R)$-space, consequently total arrivals remain bounded as previous analysis has shown. The relationship of Figs. 4 and 7 to Fig. 8 is this: The $(t_R, \Delta f_R)$-space of Fig. 8 is the transformation from (φ_1, φ_2)-space of Fig. 4 by means of the Jacobian $|J(\varphi_1, \varphi_2)/(t_R, \Delta f_R)|$; Fig. 7A represents the time rate of change of the cross-sectional area of a slice through the surface of Fig. 8 for a constant-time section and Fig. 7B is the corresponding change of cross-sectional area in the orthogonal direction. Shown also in Fig. 8 in Sec. A-A is a typical time rate of arrivals plot, and in Sec. B-B a typical doppler spectrum. In this section, finite beams for transmitting and receiving may cause intermittencies, i.e., because of beam limits, certain $t_R - \Delta f_R$ pairs are prohibited.

C. LONG PULSES

If the pulse transmitted to R and reflected is not very narrow, then conceivably arrivals at S from discrete points of x will overlap in time upon return to S. Suppose the pulse transmitted by S has duration $\Delta\tau$. An arrival at time t_R may then be a leading edge of a pulse appropriate to t_R, or to some portion of a pulse the leading edge of which occurred prior to t_R. Thus at time t_R, the rate of arrival of long pulses is

$$\left[\frac{dE(N_2)}{dt_R}\right]_{\Delta\tau} = \frac{d}{dt_R} \int_{t_R - \Delta\tau \geq t_{min}}^{t_R} \left[\frac{dE(N_2)}{dt_R}\right] dt_R \qquad (32)$$

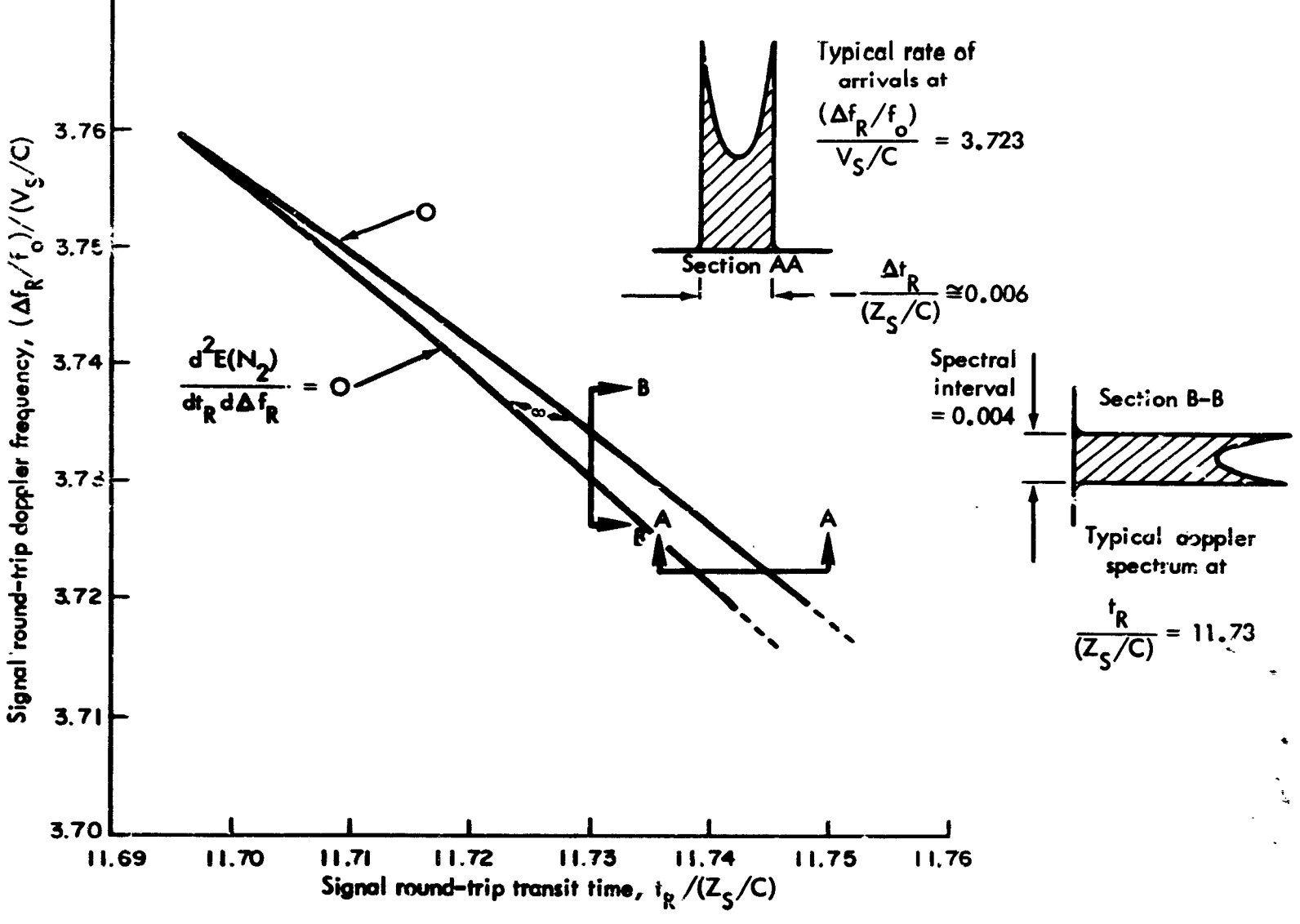

FIGURE 8 Multipath Density in Time-Frequency Space--Narrow Pulse

R2-11-66-8

where the integrand comes from Eq. 28. The expected number of discrete arrivals at S at t_R' is just the integral of Eq. 32, i.e.,

$$\left[E(N_2)\right]_{\Delta\tau} = \int_{t_R - \Delta\tau \geq t_{min}}^{t_R} \left[\frac{dE(N_2)}{dt_R}\right] dt_R$$

$$\cong \left\langle \frac{dE(N_2)}{dt_R} \right\rangle \Delta\tau \qquad (33)$$

where $\left\langle \frac{dE(N_2)}{dt_R} \right\rangle$ is a mean value of $\left[\frac{dE(N_2)}{dt_R}\right]$ during $t_R - \Delta\tau$ to t_R. Figure 9 shows an extension of Fig. 7A for a long pulse with $\Delta\tau/(z_s/\pi) = 0.004$ which for values of Eq. 8 corresponds to $\Delta\tau \cong 10.6$ msec. In Fig. 9 the maximum of $\left[E(N_2)\right]_{\Delta\tau} \cong 0.22 \left\{(z_s/\pi)^2 \left[-\frac{B_\theta''(0)}{B_\theta(0)}\right]\right\}$; thus for the typical values of Eq. 8

<u>expected number of discrete, simultaneous arrivals</u>:

$$\left[E(N_2)\right]_{\Delta\tau_{max}} = 0.22 \left\{\left(\frac{13{,}200 \text{ ft}}{\pi}\right)^2 \left(1025 \text{ ft}\right)^{-2}\right\}$$

$$= 3.7$$

i.e., at $t_R(z_s/c) \cong 11.702$, there are arrivals at S reflected from R along an expected number of 3.7 discrete paths. Referring to Eq. 33, if it is desired that no more than $[E(N_2)]_{\Delta\tau}'$ arrivals are to be expected at a given instant, then

$$\Delta\tau = \left[E(N_2)\right]_{\Delta\tau}' \Big/ \left[\frac{dE(N_2)}{dt_R}\right]_{max} \qquad (34)$$

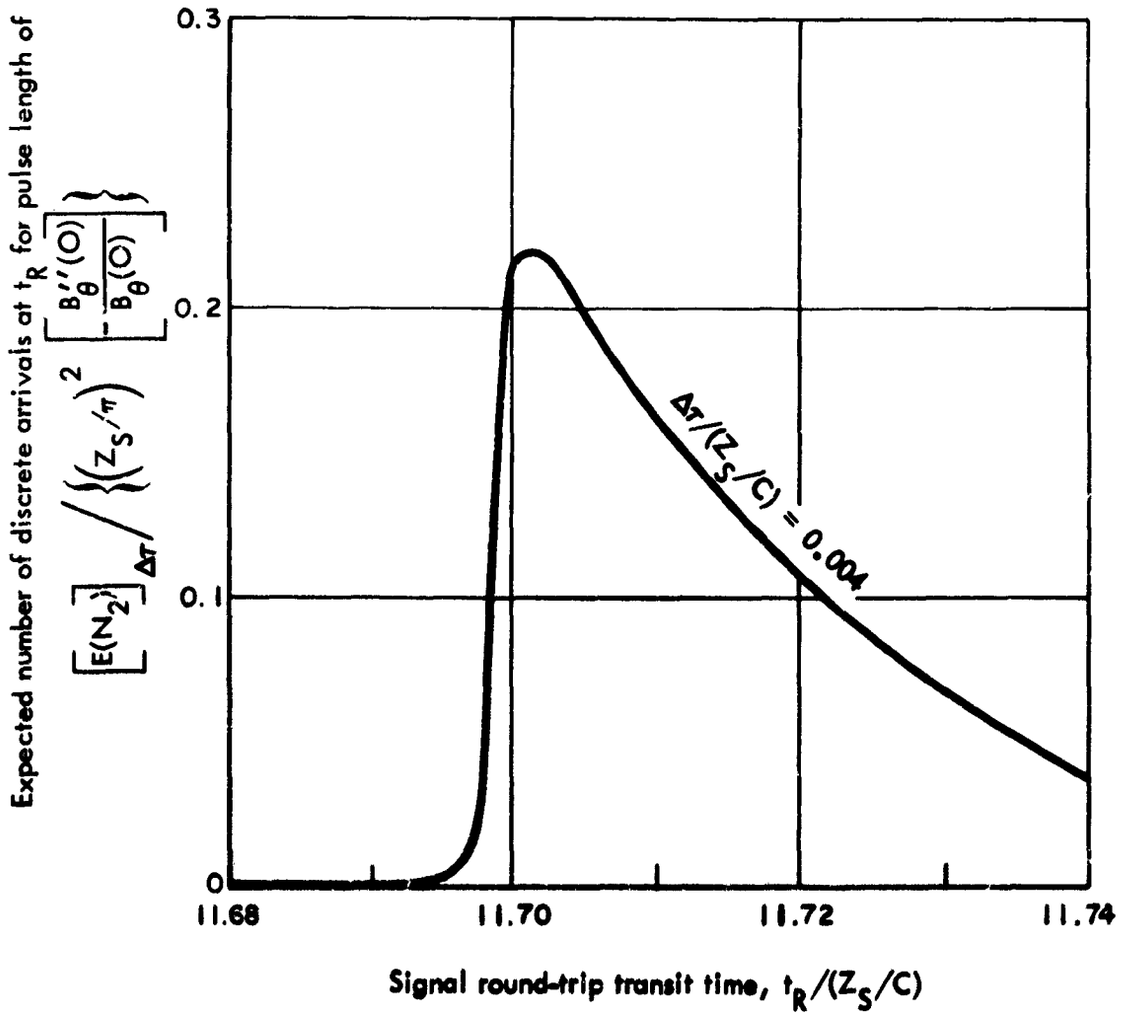

FIGURE 9 Long Pulse Discrete Arrival Density vs. Transit Time

Using Fig. 7A and the non-dimensional form of Eq. 34 gives

pulse length for a maximum of one arrival at a time:

$$\frac{\Delta\tau}{(z_s/c)} = \frac{1}{\left(\frac{z_s}{\pi}\right)^2 \left[-\frac{B_\theta''(0)}{B_\theta(0)}\right]} \Bigg/ 58 \cong 0.001$$

For the values of Eq. 8 this corresponds to $\Delta\tau = 0.001$ $\left(\frac{13{,}200 \text{ ft}}{5{,}000 \text{ fps}}\right)$ = 2.64 msec pulse length. This latter calculation gives some measure to the meaning of "narrow pulse." It appears reasonable to call a narrow pulse one such that as a function of the geometry of concern, i.e., Fig. 4, it is expected that no more than one round-trip arrival will occur at a given instant. Some intuition to the relation between pulse width, beamwidth and expected number of discrete arrivals may be gained by over-plotting on Fig. 5 time bands corresponding to pulse widths of $\Delta\tau$; the integral over the angular intervals corresponding to the time bands yields also $[E(N_R)]_{\Delta\tau}$. This is shown in Fig. 10 where transmitting and receiving beamwidths of 10 degrees centered at a depression angle of 20 degrees are included to show the truncating effect on expected arrivals due to restricted beams. Apparently from Fig. 10, after a sufficient period of time that an arbitrarily large fraction of the pulse width has passed from the (φ_1, φ_2)-space, a succeeding pulse may be transmitted with an expected degree of ambiguity resulting. Thus a basis for pulse repetition frequency is established for bottom-bounce mode of propagation of sound.

The spectral distribution of a long pulse is, with reference to Fig. 8, the integral over the surface between $(t_R - \Delta\tau)$ and t_R and an

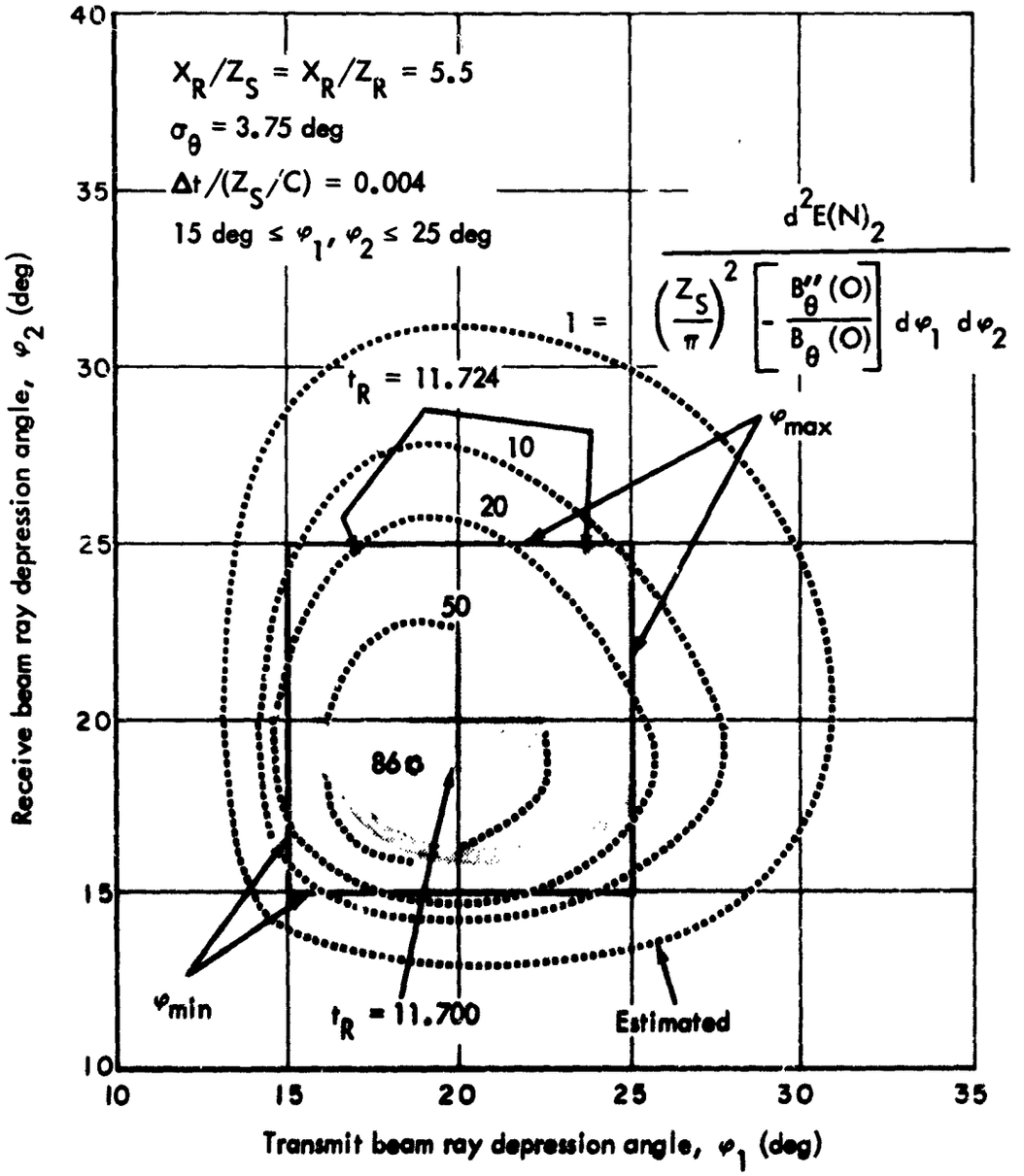

FIGURE 10 Long Pulse Display in Transmit--and Receive--Beam Angle Space

infinitesimally wide strip $d\Delta f_R$. Thus, using Eq. 31, the spectral distribution of arrivals at t_R for pulse of width $\Delta\tau$ is

$$\left[\frac{dE(N_2)}{d\Delta f_R}\right]_{\Delta\tau} = \left(\frac{z_s}{\pi}\right)^2 \left[-\frac{B''_\theta(0)}{B''_\theta(0)}\right] \int_{t_R-\Delta\tau \geq t_{min}}^{t_R} \left(\frac{dE(N_1)}{dx_1}\right)\left(\frac{dE(N_1)}{dx_2}\right)\left|J\,\frac{(x_1, x_2)}{(t_R, \Delta t_R)}\right| dt_R \quad (35)$$

Section B-B of Fig. 8 provides a basis for long pulse return spectra; the integration of Sec. B-B over $\Delta\tau$ will have a smoothing effect on the section. The resulting spectrum for pulse length of $\Delta\tau \neq 0$ will progress from that shown in the section, to one of roughly Gaussian character, then eventually to a more or less flat spectrum for very long pulses.

III. PERTURBATIONS

The analysis in the foregoing admits kinematics and bottom slopes but keeps the geometry of Fig. 4 static and assumes a planar bottom for computing θ_M and t and Δf. The error in this needs to be considered as a qualification to the analysis. Now from Eq. 2, θ_M may be written as

$$\theta_M = \frac{1}{2}\left[\varphi - \operatorname{arccot}\left(\frac{x_R}{z_R} - \frac{z_s}{z_R}\cot\varphi\right)\right] \tag{36}$$

The uncertainty in x_R arises in the motion of S and R during $\Delta\tau$, i.e., during $\Delta\tau$, x_R changes by an amount

$$\Delta x_R = (v_s + v_R)\ \Delta\tau \tag{37}$$

If $\sigma_\theta \ll 1$, $v_s \cong v_R$ and $z_s \cong z_R$ then

$$\begin{aligned}\left(x_R\right)_o - \Delta x_R &\cong 2z_s \cot\varphi_o - 2v_s\Delta\tau \\ &= 2z_s \cot\varphi_o \left[1 - \left(\frac{v_s}{c}\right)\left(\frac{\Delta\tau}{(z_s/c)}\right)\tan\varphi_o\right]\end{aligned} \tag{38}$$

where the second element in the brackets is an error term. For the typical values used previously

$$\left(\frac{v_s}{c}\right)\left(\frac{\Delta\tau}{z_s/c}\right)\tan\varphi_o = \left(0.001\right)\left(0.004\right)\left(0.364\right) \cong 0.000015$$

i.e., the fractional error in x_R due to v_s and v_R during $\Delta\tau$ is $O\left(10^{-5}\right)$. Another unrelated uncertainty arises if x_R is estimated from a knowledge of φ_o and $\langle z_s \rangle$; x_R may then be uncertain by approximately $\left(\sigma_z / \langle z_s \rangle\right)$ cot φ_o, i.e., about 400 ft for conditions of Eq. 8 (Eq. 40).

The uncertainty in z_s and z_R arises from the fact that a surface having a slope standard deviation σ_θ has also an elevation standard deviation σ_z, so that the distances of S and R above the point of reflection are uncertain in the order of σ_z. In the present problem we have assumed values of σ_θ and of $[-B''_\theta(0)/B_\theta(0)]^{\frac{1}{2}}$ and we may approximate σ_z from these.* Now, approximately

$$\sigma_\theta \cong \sigma_z / r_z \tag{39}$$

where r_z is the correlation length of bottom elevation. If $r_z = O(r_\theta) = O\left\{\left[-B''_\theta(0)/B_\theta(0)\right]^{\frac{1}{2}}\right\}$ as is likely, then

$$\sigma_z = O\left\{\sigma_\theta \left[-B''_\theta(0)/B_\theta(0)\right]^{-\frac{1}{2}}\right\} \tag{40}$$

---

*In what follows some intuitively based approximations are used. In parallel with $\theta = \arctan dz/dx \cong \Delta z/\Delta x$ if $\Delta z \ll \Delta x$, the assumption is made that $\sigma_\theta \cong \sigma_z / r_z$. Also, if for example $B_\theta(r)$ is of the form $B_\theta(r) = \sigma_\theta^2 \exp\left[-(r/r_\theta)^2\right]$, then $\left[-B''_\theta(0)/B_\theta(0)\right]^{-\frac{1}{2}} = \sqrt{2}/r_\theta$.

For the values of Eq. 8 used previously

$$\sigma_z = O\left\{\left(\frac{3.75\ \pi}{180}\right)\left(1025\ \text{ft}\right)\right\} \cong 67.5\ \text{ft}$$

and from Eq. 25, the magnitude of uncertainty in t_R is* $\Delta\tau_R/(z_s/c) \cong 2\sqrt{2}(\sigma_z/\langle z_s\rangle)\ \csc\varphi_o$ which has a typical value of 0.043. A comparison of the value $\Delta\tau_R/z_s/c = 0.043$ with the time interval of Fig. 7A shows that with 80 percent of the arrivals occurring within 0.045, importantly large time dislocations of expected arrivals occur due to bottom irregularities. Thus, for the situation in which correlation length for bottom elevation is very small compared with the ensonified interval, arrivals will occur more or less randomly in time and the standard deviation of the time uncertainty tends to be $\sigma_{t_R} \cong 2\sqrt{2}(\sigma_z/c)\ \csc\varphi_o$. Hence the situation described in Figs. 2, 3, 7A, 8, 9, and 10 and the pulse repetition frequency criterion are ideals to be hoped for but not to be expected. A more realistic estimate of arrival rate (as in Fig. 7A) of narrow pulses is described by

$$\left[\frac{dE(N_R)}{dt_{R_1}}\right]_{\sigma_z} = \frac{1}{\sqrt{2\pi}\,\sigma_{t_R}} \int_0^\infty \left[\frac{dE(N_R)}{dt_R}\right] \exp\left[-\frac{1}{2}\left(\frac{t_R - t_{R_1}}{\sigma_{t_R}}\right)^2\right] dt_R \qquad (41)$$

in which σ_{t_R} is the standard deviation of round-trip travel time $\left(\cong 2\sqrt{2}\ (\sigma_z/c)\ \csc\varphi_o\right)$ and a random normal distribution of z hence t_R is assumed. The operation of Eq. 41 tends of course to diminish the

*It is assumed that σt_R is proportional to the square root of the sums of variances of z for each leg of the round-trip path.

maximum rate of arrivals and the number of simultaneous arrivals for wide pulses and to distribute arrivals over a greater interval of time. Figure 7A contains a dashed estimate of the effect of Eq. 41 upon the $\sigma_z = 0$ case calculated there.

The effect of bottom irregularities upon doppler frequency is much less pronounced. Equation 26 shows Δf_R to be uncertain to the degree that θ_M is uncertain; this has been shown to be very small. Thus the doppler frequency distributions of Figs. 2, 3, 7B, and 8 are satisfactorily descriptive, but Fig. 8 will be smoothed as mentioned above by time-of-arrival uncertainty.

IV. CONCLUSIONS

This paper contains an analysis for determining the time of arrival and doppler frequency characteristics of a pulse transmitted to a target by reflection from a not-too-rough surface such as the sea bottom, and gives numerical values for a typical sonar application. The analysis may be important in signal processing associated with one-way transmission (communication and interference) and round-trip transmission (ranging) and in the interpretation of data from marine geophysical surveys.

The analysis shows that given sonar beam and source-target geometries, the expected number of one-way or round-trip paths between the source and target is determined primarily by the variance and correlation length of surface slope, but that the incremental time of arrival of the propagation along these paths is determined primarily by the variance of surface elevation from which slope variance derives. Contrasted to dependence of time of arrival upon surface elevation variance, doppler frequency is dependent primarily upon surface slope variance. Thus, given the relationships among variances and correlation lengths for surface elevation and some of its derivatives (p. 33), the expected number and doppler frequency characteristics are determined primarily by the slope statistics of the surface and time-of-arrival characteristics by surface elevation statistics.

Furthermore, the analysis shows a basis for maximizing or otherwise modifying the expected number of arrivals for a given beamwidth through sonar beam positioning or through tailoring of pulse length or pulse repetition frequency. A criterion for pulse length and pulse repetition frequency for bottom-bounce propagation emerges from the analysis.

Lastly, the analysis need not be restricted to the sonar problem described here, but may be applicable to ionospheric and other meteorological investigations in which reflecting or refracting centers may be in motion and source and target may or may not be moving.

REFERENCES

J.J. Martin, "Statistics of Sound Multipaths," J. ASA., 38(6), 1965, pp. 1061-2.

J.J. Martin, "Estimated Numbers of Multipaths from a Stochastic Surface--An A-Crossing Problem," Proceedings of Fifth International Congress on Acoustics, Leige, 1965. D.E. Cummins, Ed., Vol. Ib, Paper K12. Also, IDA Research Paper P-173, March 1965.

J.J. Martin, "Sea-Surface Acoustic Reverberation Theory," Appendix I, IDA Research Paper P-217, December 1965.

Peter Swerling,"Statistical Properties of the Contours of Random Surfaces," IRE Trans. Inform. Theory, IT-8, 1962, pp. 315-21.

APPENDIX I

DERIVATION OF RELATION FOR EXPECTED NUMBER OF MULTIPATHS

Consider a counting function F_d such that

$$F_d(\theta_M, \theta) = \frac{1}{d} \quad \text{when} \quad |\theta_M - \theta| \leq d/2$$

$$= 0 \quad \text{otherwise} \qquad \text{I-1}$$

where $\theta = \theta(x)$ and $\theta_M(x)$ are functions of x. Then, in the region of x of interest, i.e., Δx the number of one-way crossings N_1 will be (Ref. 4)

$$N_1 = \lim_{d \to 0} \int_{\Delta x} |\theta'| F_d(\theta_M, \theta)\, dx \qquad \text{I-2}$$

Now suppose that $\theta'(x)$ is a random process with $W(\theta_M, \theta' : x)$ as joint probability density function with θ_M. Then the expected number of crossings of (θ_M, θ), i.e., the number of one-way multipaths over a one-dimensionally rough surface is given as

$$E(N_1) = \int_{\Delta x} \int_{-\infty}^{\infty} |\theta'| W(\theta_M, \theta' : x)\, d\theta'\, dx \qquad \text{I-3}$$

Now if θ and θ' have normal distribution, then

$$E(N_1) = \frac{1}{2\pi\sigma_{\theta'}\sigma_{\theta}} \int_{\Delta x} \int_{-\infty}^{\infty} |\theta'| \exp\left[-\frac{1}{2}\left(\frac{\theta_M}{\sigma_\theta}\right)^2 + \left(\frac{\theta'}{\sigma_{\theta'}}\right)^2\right] d\theta' \, dx \qquad \text{I-4}$$

Integrating first with respect to θ' yields

$$E(N_1) = \frac{1}{\pi}\left(\frac{\sigma_{\theta'}}{\sigma_\theta}\right) \int_{\Delta x} \exp\left[-\frac{1}{2}(\theta_M/\sigma_\theta)^2\right] dx \qquad \text{I-5}$$

But if $B_\theta(r)$ is the correlation function of θ and if $B_{\theta'}(r)$ is the correlation function of θ' then it is true $B_\theta(0) = \sigma_\theta^2$ and $B_{\theta'}(0) = -B_\theta''(0) = \sigma_{\theta'}^2$, so

$$E(N_1) = \frac{1}{\pi}\left[-\frac{B_\theta''(0)}{B_\theta(0)}\right]^{\frac{1}{2}} \int_{\Delta x} \exp\left[-\frac{1}{2}(\theta_M/\sigma_\theta)^2\right] dx \qquad \text{I-6}$$

In a similar way, the expected number of one-way multipaths for two-dimensional roughness is (Ref. 2)

$$\left[E(N_1)\right]_{2D} = \frac{1}{\pi}\left[-\frac{B_\theta''(0)}{B_\theta(0)}\right]^{\frac{1}{2}}\left[-\frac{B_\vartheta''(0)}{B_\vartheta(0)}\right]^{\frac{1}{2}} \int_{\Delta x}\int_{\Delta y} \exp\left[-\frac{\theta_M^2}{2\sigma_\theta^2} - \frac{\vartheta_M^2}{2\sigma_\vartheta^2}\right] dxdy \qquad \text{I-7}$$

in which $\vartheta_M = \delta_M(x,y)$ and for round-trip multipaths for two-dimensional roughness

$$\left[E(N_2)\right]_{2D} = \frac{1}{\pi^4}\left[-\frac{B''_\theta(0)}{B_\theta(0)}\right]\left[-\frac{B''_\vartheta(0)}{B_\vartheta(0)}\right]\int_{\Delta x_1}\int_{\Delta x_2}\int_{\Delta y_1}\int_{\Delta y_2}$$

$$\exp\left\{-\frac{1}{2}\left[\left(\frac{\theta_M}{\sigma_\theta}\right)_1^2 + \left(\frac{\theta_M}{\sigma_\theta}\right)_2^2 + \left(\frac{\vartheta_M}{\sigma_\vartheta}\right)_1^2 + \left(\frac{\vartheta_M}{\sigma_\vartheta}\right)_2^2\right]\right\} dx_1\, dx_2\, dy_1\, dy_2 \qquad \text{I-8}$$

and this could of course be elaborated to round trips over two-dimensionally rough surfaces bounding both surface and bottom, in which case an eight-fold integral would result (Ref. 2).

What has gone before assumes θ is randomly distributed and z is precisely known, which may not be true. If θ and z are simultaneously uncertain then the counting function becomes for $z = \bar{z} - \epsilon$

$$F_d(\theta, z) = \frac{1}{d} \quad \text{when} \quad \left|\cot(\varphi - 2\theta) - \frac{x_R - (\langle z_S\rangle - \epsilon)\cot\varphi}{(\langle z_M\rangle - \epsilon)}\right| \le \frac{d}{2} \qquad \text{I-9}$$

$$= 0 \quad \text{otherwise}$$

In this event $E(N_1)$ becomes (for $z' \cong \theta$)

$$E(N_1) = \int\int\int\int \left|\frac{d}{dx}\left\{\cot[\varphi - 2\theta] - \frac{x_R - [\langle z_S\rangle - \epsilon(x)]\cot\varphi}{[\langle z_R\rangle - \epsilon(x)]}\right\}\right| \qquad \text{I-10}$$

$$\cdot\, W[z, \theta, \theta' : x(\varphi)]\, dz\, d\theta\, d\theta'\, dx$$

integrated over the whole domain of z, θ, θ' and x. The complexity of this for the purpose of evaluation makes the approximate approach of Eq. 41 appealing.

APPENDIX II

DOPPLER FREQUENCY RELATIONSHIPS

Let Fig. II-1 be used to represent doppler frequency for both one-way and round-trip paths. For the one-way path if f_o is the at-rest radiation frequency of S then the frequency f_1 received at R is*

$$\frac{f_1}{f_o} = \frac{1 + (v_R/c) \cos (\varphi_1 - 2\theta_1)}{1 - (v_s/c) \cos \varphi_1} \qquad \text{II-1}$$

If $v_s/c \ll 1$ and $v_R/c \ll 1$, as is usual, then

$$\frac{\Delta f_1}{f_o} = \frac{f_1 - f_o}{f_o} \cong (v_s/c) \cos \varphi_1 + (v_R/c) \cos (\varphi_1 - 2\theta_1) \qquad \text{II-2}$$

In the round-trip case, the velocity v_R may be resolved into a component bisecting the arriving and returning rays, in which case, using the approximation just developed

$$\left(\frac{\Delta f}{f_o}\right)_R \cong (v_s/c) \cos \varphi_1 + (v_s/c) \cos \varphi_2 \qquad \text{II-3}$$

$$+ 2(v_R/c) \cos \left\{\frac{1}{2}\left[(\varphi_2 - 2\theta_2) + (\varphi_1 - 2\theta_1)\right]\right\} \cos \left\{\frac{1}{2}\left[(\varphi_2 - 2\theta_2) - (\varphi_1 - 2\theta_1)\right]\right\}$$

*See, for example, any elementary physics text.

Applying suitable trigonometric identities to this gives

$$(\Delta f_R/f_o) = (v_s/c)\cos\varphi_1 + (v_R/c)\cos(\varphi_1 - 2\theta_1) + (v_s/c)\cos\varphi_2 + (v_R/c)\cos(\varphi_2 - 2\theta_2) \qquad \text{II-4}$$

that is, for the round-trip case it is as if a doppler frequency

$$\left[\frac{(\Delta f_i/f_o)}{(v_s/c)}\right] = \cos\varphi_i + (v_R/v_s)\cos(\varphi_i - 2\theta_i),\ i = 1,2 \qquad \text{II-5}$$

may be associated with each leg of the round-trip path.

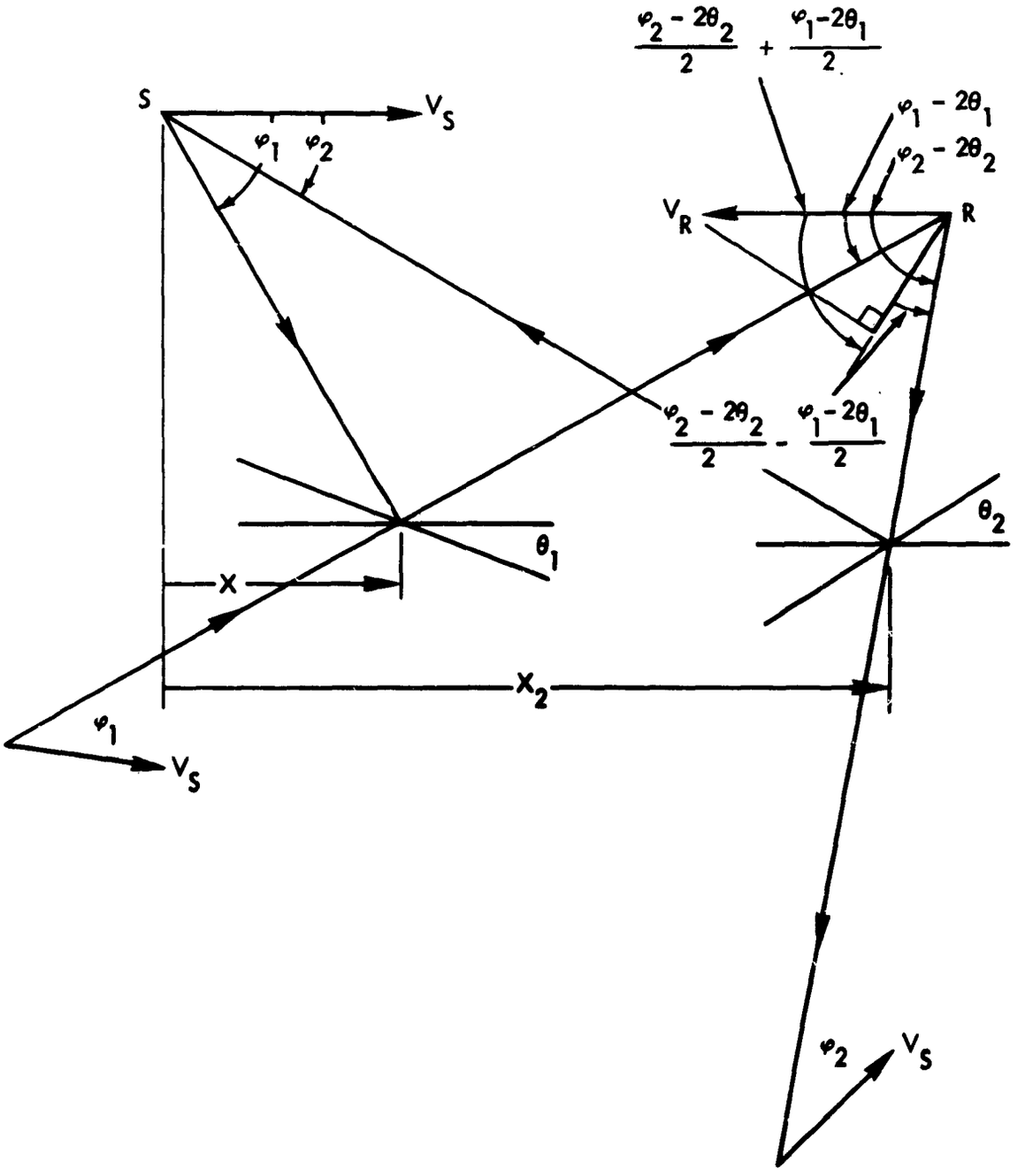

FIGURE II-1 Doppler Frequency Calculation Geometry

Security Classification

DOCUMENT CONTROL DATA - R&D

(Security classification of title, body of abstract and indexing annotation must be entered when the overall report is classified)

1 ORIGINATING ACTIVITY (Corporate author)	2a. REPORT SECURITY CLASSIFICATION
Institute for Defense Analyses	Unclassified
	2b GROUP

3 REPORT TITLE

Time and Frequency Characteristics of an Acoustic Signal Reflected from a Rough Boundary

4 DESCRIPTIVE NOTES (Type of report and inclusive dates)

Research Paper P-243 -- February 1966

5 AUTHOR(S) (Last name, first name, initial)

Martin, John J.

6 REPORT DATE	7a. TOTAL NO. OF PAGES	7b. NO. OF REFS
February 1966	50	4

8a. CONTRACT OR GRANT NO.	9a. ORIGINATOR'S REPORT NUMBER(S)
SD-50	
b. PROJECT NO. T-37	Research Paper P-243
c	9b. OTHER REPORT NO(S) (Any other numbers that may be assigned this report)
d	IDA/HQ 66-4568

10. AVAILABILITY/LIMITATION NOTICES

Distribution of this document is unlimited.

11. SUPPLEMENTARY NOTES	12. SPONSORING MILITARY ACTIVITY

13. ABSTRACT

This paper contains an analysis for determining the time of arrival and doppler frequency characteristics of a pulse transmitted to a target by reflection from a not-too-rough surface such as the sea bottom, and gives numerical values for a typical sonar application. The analysis may be important in sonar signal processing associated with one-way or round-trip transmission and in the interpretation of data from marine geophysical surveys; it may in addition have application to propagation of electro-mechanical waves by ionospheric refraction.

DD FORM 1 JAN 64 1473

Security Classification